Available online at www.sciencedirect.com
ScienceDirect
Journal of Magnetic Resonance 188 (2007) 168–175
JMR Journal of Magnetic Resonance
www.elsevier.com/locate/jmr

Communication

Imaging contrast effects in alginate microbeads containing trapped emulsion droplets

Holly J. Hester-Reilly, Nina C. Shapley *

Department of Chemical Engineering, Columbia University, 500 W. 120th Street, MC 4721, New York, NY 10027, USA

Received 21 March 2007; revised 11 May 2007
Available online 15 June 2007

Abstract

This study focuses on spherical microparticles made of cross-linked alginate gel and microcapsules composed of an oil-in-water emulsion where the continuous aqueous phase is cross-linked into an alginate gel matrix. We have investigated the use of these easily manufactured microbeads as contrast agents for the study of the flow properties of fluids using nuclear magnetic resonance imaging. Results demonstrate that combined spin–spin (T_2) relaxation and diffusion contrast in proton NMR imaging can be used to distinguish among rigid polymer particles, plain alginate beads, and alginate emulsion beads. Multi-echo CPMG spin-echo imaging indicates that the average spin–lattice (T_1) and spin–spin (T_2) relaxation times of the plain alginate and alginate emulsion beads are comparable. Meanwhile, diffusion-weighted imaging produces sharp contrast between the two types of alginate beads, due to restricted diffusion inside the embedded oil droplets of the alginate emulsion beads. While the signal obtained from most materials is severely attenuated under applied diffusion gradients, the alginate emulsion beads maintain signal strength. The alginate emulsion beads were added to a suspension and imaged in an abrupt, annular expansion flow. The emulsion beads could be clearly distinguished from the surrounding suspending fluid and rigid polystyrene particles, through either T_2 relaxation or diffusion contrast. Such a capability allows future use of the alginate emulsion beads as tracer particles and as one particle type among many in a multimodal suspension where detailed concentration profiles or particle size separation must be quantified during flow.

Keywords: Alginate; Particle; Emulsion; Suspension; Contrast agent; Flow; Tracer

1. Introduction

Alginate, a natural polysaccharide, is a useful material with applications in various industries including food, cosmetics, pharmaceuticals, and medical devices. In the presence of multivalent cations such as calcium ions, alginate cross-links to form gels [1]. Some specific uses of cross-linked alginate include the protection and controlled delivery of probiotic bacteria [2,3], enzymes [4], genes [5], and small molecule and protein drugs [1,6], and the removal of heavy metal ions from water [7].

In this study, we created microbeads made of cross-linked alginate gel and microcapsules composed of an oil-in-water emulsion where the continuous aqueous phase was cross-linked into an alginate gel matrix. We have investigated the use of these microbeads as contrast agents for the study of the flow properties of fluids using proton nuclear magnetic resonance (NMR) imaging. The advantages of working with alginate beads include the ease of manufacture, gentle production conditions [8], potential for microencapsulation [9], established biocompatibility [4,10], and well characterized NMR properties [11–13].

The flow properties of fluids are of considerable interest in the materials processing industries and in the fields of chemical engineering and biomaterials. Magnetic resonance is a proven technique for measuring the rheology of such materials. While well known standard paramagnetic contrast agents differentiate parts of the sample by altering local NMR relaxation times, the alginate beads containing emulsion droplets create contrast based on diffusion properties. Under applied diffusion gradients, the

* Corresponding author. Fax: +1 212 854 3054.
E-mail address: ncs2101@columbia.edu (N.C. Shapley).

1090-7807/$ - see front matter © 2007 Elsevier Inc. All rights reserved.
doi:10.1016/j.jmr.2007.05.022

signal from plain alginate gel beads and from liquids is sharply attenuated, as to be almost undetectable. However, the corresponding signal from alginate emulsion beads remains only slightly attenuated, due to restricted diffusion of the confined oil molecules inside the droplets which are embedded in the particles [14,15].

The concept of a positive contrast agent, with a long-lasting signal, is attractive for certain applications, such as the NMR velocimetry of fluid flows by phase encoding [16,17]. Tracking of a contrast agent in the form of tracer particles can provide information about the flow field. Fluid filled particles and natural seeds have been utilized in dry granular flow systems [18,19]. However, few studies have involved tracer particles with diffusion based contrast. Wassenius et al. developed polymeric (PMMA) core-shell tracer particles containing liquid hexadecane in order to extend the lower limit of phase encoding velocity measurements to extremely slow flows [20–22]. The authors were the first to exploit restricted diffusion effects in a tracer particle. Meanwhile, alginate emulsion beads were employed in a previous study by Noth et al. [23] where perfluorocarbon oil droplets were encapsulated and the spin–lattice (T_1) relaxation time of the ^{19}F NMR signal was used as an oxygen sensor in vivo. The alginate emulsion beads were produced by rapid ionic gelation and did not require detailed chemical synthesis. To our knowledge, the work described here represents the first use of alginate beads with embedded oil droplets for contrast in diffusion weighted imaging.

In this paper, we demonstrate that combined spin–spin (T_2) relaxation and diffusion contrast can be used to distinguish among rigid polymer particles, plain alginate beads, and alginate emulsion beads. Such a capability allows future use of the alginate emulsion beads as tracer particles and also as one particle type among many in a multimodal suspension where detailed concentration profiles or particle size separation must be quantified during flow.

2. Experimental

2.1. Plain alginate bead preparation

Sodium alginate (Acros Organics, Geel, Belgium) was dissolved in water at a concentration of 2 wt%. According to the manufacturer, the alginate, which is a copolymer, contained 65–75% guluronic acid (G) subunits and 25–35% mannuronic acid (M) subunits, and had a molecular weight of 450–550 kDa, specifically with a viscosity of 485 cP for a 1 wt% aqueous solution. The 2 wt% alginate solution also contained a 0.2 M concentration of NaCl in order to promote the formation of homogenous beads [12]. A bath of 0.1 M $CaCl_2$ (Amend, Irvington, NJ) was prepared, and NaCl was also added to the bath to yield a 0.075 M concentration. Using a syringe pump equipped with a 5 cc syringe and a 30G 1/2 needle angled downward, the alginate solution was dropped into the bath of calcium chloride and sodium chloride solution at a volumetric flow rate of 0.10 mL/min and from a height of 12 cm. The setup is shown in Fig. 1. The bath was stirred manually and the beads were allowed to equilibrate for a minimum of 15 min to allow the cross-linking to complete. The completed beads were stored in deionized water.

2.2. Emulsion bead preparation

To make the emulsions for the alginate emulsion beads, isooctane, 1,6 dibromohexane (both from Fisher Chemical, Fairlawn, NJ), Tween-20 surfactant (polyoxyethylene 20-sorbitan monolaurate, Fisher BioReagents, Fairlawn, NJ), and water were combined in an Erlenmeyer flask and blended at 15,000 rpm for 3 min using a T 25 digital Ultra-Turrax homogenizer (IKA Works, Inc., Wilmington, NC). The mixture was composed of 0.8 wt% Tween-20, 21.5 wt% isooctane, 21.5 wt% 1,6 dibromohexane, and 56.2 wt% water. The oil phase was made of a mixture of 1,6 dibromohexane and isooctane in order to match the density of the beads and the suspending fluid. Separately, powdered sodium alginate was dissolved in water at a concentration of 5.5 wt%. The sodium alginate solution and the oil-in-water emulsion were then added together and allowed to equilibrate overnight. The final recipe of the emulsion beads was 1.6 wt% sodium alginate, 0.5 wt% Tween-20, 14.2 wt% isooctane, 14.3 wt% 1,6 dibromohexane, and 69.3 wt% water. Finally, the emulsion was stirred for 30 min on a stir-plate.

To produce the emulsion beads, the same syringe pump setup was used as for the plain alginate beads. Storage times prior to imaging varied from 1 day to 1 month. Although we did not image emulsion beads after longer periods of time, the emulsions appear to remain stable for over a year after the manufacture of the beads. It has been noted previously that cross-linking of the aqueous phase leads to long term stability of the emulsion [23]. Final bead diameter was an average of 1.5 mm. It may be noted, however, that other bead diameters are obtainable via this method. Altering the concentration of the alginate and thus the viscosity of the solution will change the bead diameter, where a higher viscosity leads to a larger bead diameter [24]. Additionally, adding an air flow that streams

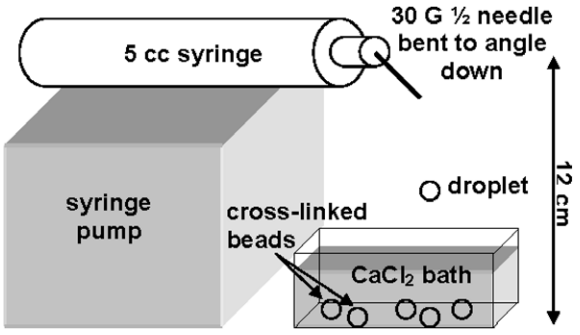

Fig. 1. Schematic view of syringe pump, needle, and cross-linking bath for bead production.

past the needle tip will result in smaller bead diameters, ranging from 300 μm to 1.5 mm [12].

2.3. Suspension preparation

A suspension consisting of rigid, spherical particles in a Newtonian fluid and incorporating the alginate emulsion beads as tracer particles was prepared. The emulsion beads were added at a concentration of 2.4 wt% to a suspension made of 20.6% volume fraction polystyrene spheres (PB-2, Maxi-Blast Inc., South Bend, IN) with a mean diameter of 485 ± 105 μm suspended in a mixture of glycerin (9.3 wt%), water (90.2 wt%), and hydroxyethylcellulose (HEC, 0.5 wt%, Natrosol MR, Aqualon Group, Hercules Inc., Wilmington, DE).

2.4. Nuclear magnetic resonance imaging

Images of the beads were taken using a 9.4 T vertical bore magnet (Bruker WB 400). To compare the particle properties, the emulsion beads, the plain alginate beads, and the polystyrene particles were imaged together. Each type of beads was loaded separately into an Eppendorf tube (1.5 mL), surrounded by deionized water. The beads were packed tightly into the Eppendorf tubes so that rising or settling of the beads due to density differences relative to the water was eliminated. The three Eppendorf tubes were then placed inside a large, water-filled centrifuge tube so that they were loaded inside the magnet simultaneously. To assist in the set-up, the Eppendorf tubes were taped together, which is apparent in some of the images.

Finally, to test the feasibility of implementing the emulsion beads as tracer particles, the beads were added to a suspension of rigid polystyrene particles undergoing flow through a 4:1:4 abrupt, annular contraction–expansion. The flow loop and operating conditions are described in Moraczewski et al. [25,26]. The suspensions, prepared as described above, were loaded into the flow cell, and imaged at the site of the expansion section of the flow.

In all of the experimental set-ups, multiple types of images were obtained. Spin-echo intensity images were recorded in both the transverse and longitudinal directions. To determine the spin–spin (T_2) relaxation time of the beads, multiple CPMG spin-echo images were acquired at increasing echo times. Additionally, diffusion images were obtained using stimulated echo diffusion weighted imaging. All images had a 3 cm × 3 cm field of view and contained 128×128 pixel. Also, each image was obtained from a single scan. Slice thickness values ranged from 0.5 mm to 2 mm. Accordingly, the image usually contains only a slice of an entire bead. In this situation it can be assumed that the effects of volume averaging are negligible, except at the edges of the beads.

2.5. Data analysis

To quantify the T_2 relaxation time of the beads, the intensity value was plotted as a function of echo time and the data were fit to a single exponential decay curve using a least squares analysis. For the T_2 map, this analysis was applied to each pixel of the image using a Matlab 7.0 program. For the graphs in Figs. 3 and 5, a pixel was selected at the center of a bead, and the data was acquired for that pixel at each echo time. This was repeated four more times and then the signal intensities were averaged over all five of the measured pixels. These averaged intensities were then fit by an exponential decay curve. Basic viewing of the images, selection of pixels, and acquisition of data values for a given pixel were accomplished using the "stacks" function of ImageJ 1.36b.

3. Results and discussion

To compare the properties of several types of particles, the alginate emulsion beads, the plain alginate beads, and the rigid polystyrene particles were packed into vials and imaged together, while surrounded by deionized water. Fig. 2 consists of three transverse images of the same set of vials. Figs. 2(a) and (b) were obtained from a multi-echo CPMG scan that acquired 25 spin-echo images at increasing echo times from 5.37 ms to 134 ms. The CPMG pulse sequence implemented here is quite similar to the one presented by Edzes et al. [27]. The slice thickness of the image was 0.5 mm, and the repetition time was 2 s. Fig. 2(a) shows a spin-echo image with an echo time of 37.59 ms, showing the sample morphology and contrast in intensity among the solid polystyrene spheres, the alginate emulsion gel beads, and the plain alginate gel beads.

Fig. 2(b) shows a map of the spin–spin (T_2) relaxation time, calculated from the entire series of multi-echo images. To create the T_2 map, a Matlab 7.0 program compiled the data from the 25 images into curves of intensity versus echo time. Then, the T_2 relaxation time was obtained from curve fitting for each pixel of the 128×128 pixel image. In Fig. 2(b) it can be seen that the T_2 range for the plain alginate beads is 50 ± 20 ms (scale from 0 ms to 100 ms), and the T_2 range for the emulsion beads is comparable at 60 ± 20 ms, while the water at the center of the large tube shows the longest relaxation time of approximately 670 ± 35 ms. The signal from the rigid polystyrene beads decays too rapidly to be detected at a significant level.

A lower spin–spin (T_2) relaxation time tends to indicate lower mobility of protons in the material and hence a more solid-like environment [12], where the gel particles have intermediate properties between those of rigid polymer particles and of free water. According to Simpson et al. [13] and McConville and Pope [28], the majority of the proton signal and T_2 relaxation observed from the beads arises from water within the gel, where there is reduced translational mobility of free water due to the pore structure of the gel, and exchange occurs between free and bound water protons. In the alginate emulsion beads, the oil droplets contribute to the proton signal as well, but the T_2 relaxation is dominated by the continuous phase, which is an aqueous hydrogel. T_2 mapping provides strong contrast

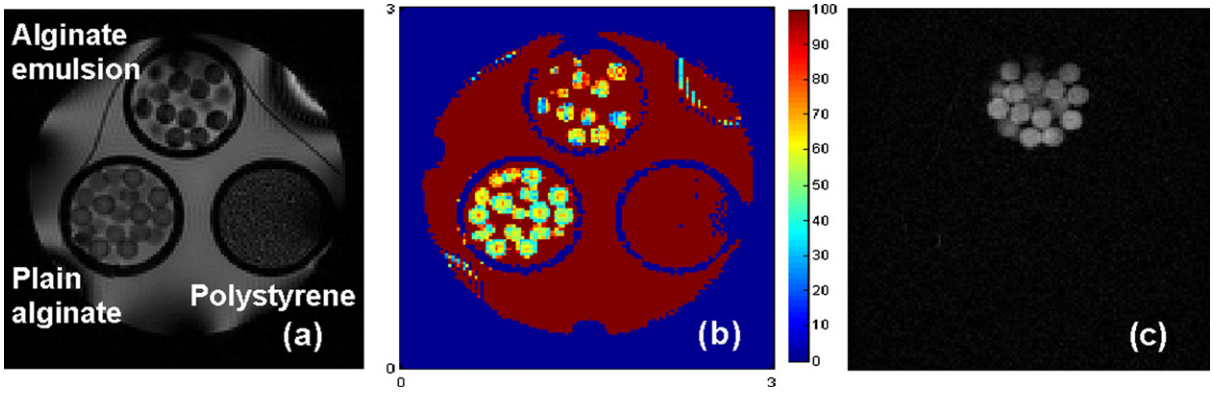

Fig. 2. Transverse images of three vials containing rigid polystyrene particles, plain alginate beads, and oil-in-water alginate emulsion beads, each surrounded by water. The vials are taped together inside a larger, water-filled centrifuge tube. All three images have FOV = 3 cm × 3 cm, 128 × 128 pixel. (a) Spin-echo image obtained from CPMG series, with TR = 2 s, TE = 37.59 ms, slice thickness = 0.5 mm; (b) T_2 relaxation time map (scale indicates 0–100 ms). CPMG pulse sequence with TR = 2 s, TE = 5.37 ms, 25 echoes, slice thickness = 0.5 mm; and (c) stimulated echo diffusion weighted image acquired at a diffusion gradient strength of 200 mT/m, TR = 2 s, TE = 11.5 ms, $\Delta = 400$ ms, $\delta = 1$ ms, slice thickness = 1.5 mm.

between the alginate beads, both plain and emulsion, the polystyrene beads, and the water.

Edzes et al. [27] point out that the CPMG pulse sequence, also utilized here, does not compensate for apparent additional relaxation resulting from diffusion and susceptibility effects. In our system, which consisted only of polymers and oil and water, where all particles were surrounded by water, magnetic susceptibility inhomogeneities were minimal. The additional signal decay caused by diffusion, according to Eq. (6) of Edzes et al. [27] was significant for the slowly relaxing liquid water, but was negligible for both types of alginate gel particles. If the observed T_2 relaxation time of the water (670 ± 35 ms for the water at the center of the large tube) is corrected to account for diffusion effects, the corrected T_2 is 875 ± 60 ms. The observed and the corrected values for T_2 of water are comparable to the range of values obtained by Simpson et al. at 17.6 T (579 ± 66 ms) [13] and by Potter et al. at 2.0 T (~800 ms). [11].

Finally, a stimulated echo diffusion weighted image sequence was applied to the same three vials. The pulse sequence is identical to the one presented in the work of d'Avila et al. Fig. 2, [29]. Each image was collected with a repetition time of 2 s and an echo time of 11.5 ms. The diffusion time (Δ) for each image was 400 ms and the gradient duration (δ) was 1 ms. The slice thickness was 1.5 mm, equivalent to the average diameter of the beads, and seven images were recorded with diffusion gradients ranging from 5 mT/m to 200 mT/m. Fig. 2(c) shows the image acquired at a diffusion gradient strength of 200 mT/m. The oil molecules confined inside the emulsion droplets can only undergo small displacements (i.e. restricted diffusion), and thus the diffusion weighted image shows a bright, minimally attenuated signal for the emulsion beads [30]. Even at a low diffusion gradient strength of 5 mT/m, the alginate emulsion beads have approximately twice the average signal intensity of the pure water. The emulsion bead/water intensity ratio increases to at least a factor of five at 100 mT/m and a factor of 10–20 at 200 mT/m. Hence, the image in Fig. 2(c) demonstrates the feasibility of employing the emulsion beads as a contrast agent through the use of diffusion imaging.

In Fig. 3, the average signal intensities of the plain alginate beads, the alginate emulsion beads, the polystyrene particles, and the water surrounding the three small vials are plotted on a graph to demonstrate the contrast in signal intensity and T_2 relaxation between the various materials. The signal intensities are taken from the same run that produced the images in Figs. 2(a) and (b), and they are plotted over the 25 echo times ranging from 5.37 ms to 134 ms.

The average T_2 relaxation times of the various beads and the water were calculated by fitting a single exponential function[11] to each set of data shown in Fig. 3. The longest T_2 relaxation times were found for water (averaged over the entire large tube) and polystyrene particles in

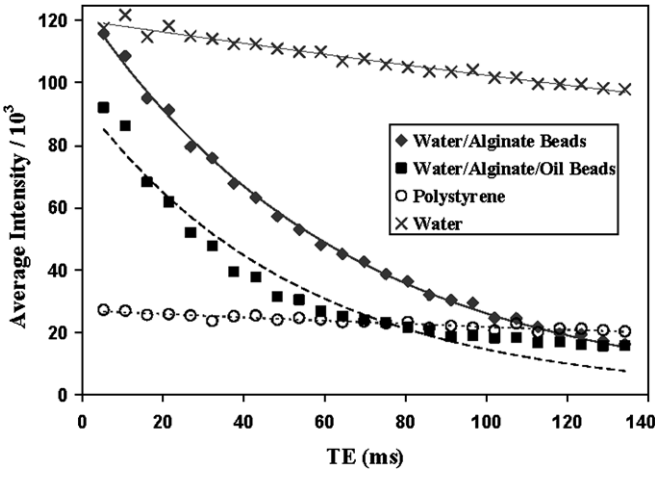

Fig. 3. Average signal intensity, in thousands, of several bead compositions at echo times ranging from 5.37 ms to 134 ms, from a multi-echo CPMG spin-echo sequence shown in Fig. 2(a) and (b). The lines are single exponential curve fits.

water, with values of 631 ms and 462 ms, respectively. Since the T_2 relaxation time for rigid solids is typically 1 ms or less, the value obtained for the polystyrene likely arises from the surrounding water, which may have been slightly restricted by the narrow spacing of the densely packed polystyrene particles. The plain alginate beads and the alginate emulsion beads exhibited an order of magnitude shorter T_2 relaxation times, providing strong T_2 contrast from the water and the polystyrene in water. The centers of the plain alginate beads in this run exhibited a T_2 relaxation time of 64.0 ms, and the centers of the alginate emulsion beads exhibited a T_2 relaxation time of 53.8 ms.

To determine if the materials presented contrasting spin–lattice (T_1) relaxation behavior, images were acquired with various repetition times, following the procedure described by Simpson et al. [13] The repetition time TR ranged from 250 ms to 3000 ms, while the other parameters were held constant. Average intensity values of the water, plain alginate beads, and alginate emulsion beads in each image were normalized by the maximum intensity value of the image. Saturation of the water signal was apparent for TR < 1 s. However, saturation was not observed in the signal from the plain alginate beads or alginate emulsion beads at the TR values tested. Qualitatively, these results suggest that the T_1 relaxation time is slightly lower in the alginate gel beads than in the water. Previously, Simpson et al. [13] reported that alginate gel and pure water did not display significantly different T_1 relaxation behavior. However, the molecular weight of the alginate used in this study was at least twice the molecular weight of the alginate examined by Simpson et al. The higher molecular weight of the alginate can lead to a higher density of entanglements in the gel, resulting in higher cross-link density and smaller pore sizes, which can influence the T_1 relaxation time. The molecular weight difference can explain the greater impact of cross-linked alginate on T_1 observed in this study compared to the study by Simpson et al.

The plain alginate beads were imaged both within 3 days of being made, 1 month later, and again approximately 4 months later, after being stored in water for the duration. Fig. 4 shows the difference in the composition of the beads that can be seen in the T_2 map. Fig. 4(a) and (b) show a spin-echo image and T_2 map of the plain alginate beads taken within 3 days of being made. In Fig. 4(b), each bead has a nearly homogenous T_2 value of 33 ± 10 ms across its interior, while slightly longer relaxation times are visible around the edges of the beads. The enhanced T_2 values observed at the edges of the beads can be explained by the averaging of water as well as alginate gel over the finite slice thickness and finite pixel size of the image, in regions where the bead thickness is small, and the pixel area may include both gel and water.

The observed T_2 value of 33 ± 10 ms for the plain alginate beads shown in Fig. 4(b) is smaller than the value obtained by Simpson et al. [13] of 80 ms for alginate with a similar subunit ratio of 73% G. As discussed above in the comparison of T_1 properties, we attribute the difference in T_2 relaxation times between the two studies to the difference in molecular weight, by at least a factor of two, of the alginate polymers. The high molecular weight alginate used in this study is likely to produce a densely cross-linked gel, which results in more solid-like properties (i.e. shorter relaxation times) compared to the low molecular weight cases presented in Simpson et al. [13].

The imaging procedure was repeated one month later for the same sample and the results are shown in Fig. 4(c) and (d). From the T_2 map presented in Fig. 4(d), it is clear that the relaxation time of the plain alginate beads did not change appreciably, while the adjacent water showed a dramatic decrease in the relaxation time.

In Fig. 4(e) and (f), a spin-echo image and T_2 map of the plain alginate beads after being stored in water for approximately 4 months are shown. Note that these are the same images appearing in Fig. 2(a) and (b). Fig. 4(f) shows that at the center of the beads, the spin–spin relaxation time is significantly increased from that of the same beads 3 and 4 months earlier. The interiors of the beads appear to have T_2 values between 65 ms and 75 ms (the scale indicates 0–100 ms), while the outer portions of the beads have T_2 values ranging from about 40 ms to 50 ms. The mean relaxation times of the stored beads significantly increased to 50 ± 20 ms from the initial reading of about 33 ± 10 ms for the homogenous beads immediately after creation. The change observed was not homogeneous, but was more pronounced in the cores of the beads, effectively turning the particles into capsules.

In addition, the relaxation time of the adjacent water inside the plain alginate bead vial changed over time. The relaxation time of the interstitial water is much lower (115 ± 15 ms) for the fresh beads, 3 days after production, than for pure water (670 ± 35 ms). There is a further decrease observed in the relaxation time of the interstitial water over the following month, to 70 ± 5 ms. For the stored beads, imaged after 4 months, fresh water was added to the small vial before imaging, and the T_2 relaxation time is identical to that of the water outside the three vials. The observation of increasing water mobility and fluidity inside the beads over time, coupled with the decreasing relaxation time of the surrounding water, suggests that leaching of calcium ions into the solution, perhaps after incomplete gelation in the bead cores [12], occurred soon after bead production, continued over the subsequent month, and was followed by the swelling of the alginate gel in the bead interiors.

The change in bead properties over time is demonstrated further in Fig. 5, which contains a graph comparing the average intensity versus the echo times of the plain alginate beads within days of being made and 4 months later. The graph shows that the signal decay time was shorter when the beads were fresh (see Fig. 4(a) and (b)) than when the beads were imaged 4 months later (see Fig. 4(e) and (f)). The average T_2 value of the bead centers within 3 days of production was also calculated based on the data shown

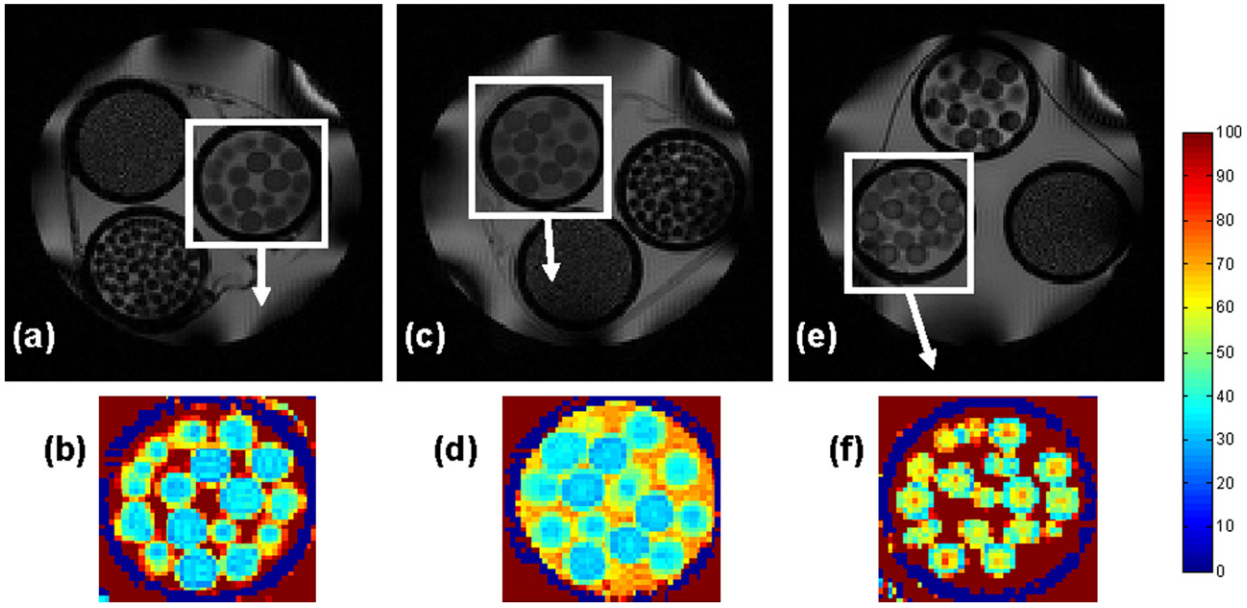

Fig. 4. Spin-echo images and corresponding T_2 relaxation time maps (ms) of plain alginate beads: (a, b) within 3 days of production; (c, d) after 1 month of storage in water; (e, f) after 4 months of storage in water, with fresh water added to the vial (the same sample shown in Fig. 2). The T_2 relaxation time maps (b), (d), (f) were obtained from a CPMG pulse sequence with TR = 2 s, TE = 5.37 ms, 25 echoes, FOV = 3 cm × 3 cm, 128 × 128 pixel, slice thickness = 0.5 mm. The region of interest shown is the plain alginate bead vial. The spin-echo images (a), (c), (e) are sample images from these sequences, with TE = 37.59 ms.

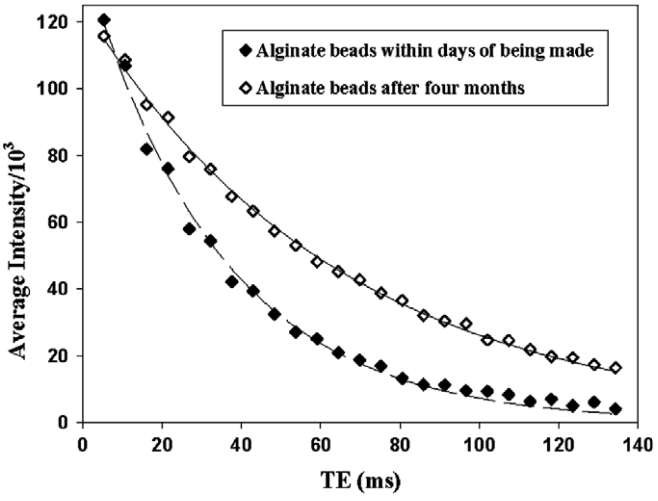

Fig. 5. Relaxation curves of plain alginate beads, tested within 3 days of manufacture (closed symbols) and also 4 months later (open symbols). Data points show the average signal intensity, in thousands, versus echo time from a multi-echo CPMG spin-echo sequence shown in Fig. 4(a), (b), (e) and (f). The lines are single exponential curve fits.

in Fig. 5, and was found to be 33.8 ms. The average T_2 relaxation time of the same bead centers 4 months later was 64.0 ms, nearly double the initial relaxation time, suggesting significant degradation of the plain alginate beads over time.

For the emulsion beads, the change over one month between Fig. 4(a) and (b) and Fig. 4(c) and (d) was less marked than for the plain alginate beads. In Fig. 4(b), within 3 days after production, the emulsion beads had the same T_2 relaxation time value of 33 ± 10 ms as the plain alginate beads, and the interstitial water for the emulsion beads had a broad T_2 relaxation time distribution of 210 ± 35 ms. The higher water relaxation time suggests that the initial leaching of calcium ions from the emulsion beads was slower than that from the plain alginate beads. One month later, the range of emulsion bead T_2 relaxation times broadened to 33 ± 20 ms and the water relaxation time did not change significantly. Over the month observed, the emulsion beads became more nonuniform, but the extent of the change in the adjacent water was less pronounced than that detected in the plain alginate vial, suggesting a slower progression of ion leaching compared to the plain alginate beads. The emulsion beads appear to be more stable than the plain alginate beads, although further observation is needed to confirm this conclusion.

To demonstrate the imaging contrast effects of the emulsion beads in a flow experiment, a 2.4 wt% concentration of emulsion beads was added to a suspension with 20.5% volume fraction rigid polystyrene particles of 485 ± 105 μm diameter. The polystyrene particles have been used in multiple NMR flow experiments [25,26]. Fig. 6 shows longitudinal images of the suspension as it experienced a contraction–expansion flow. The suspension was pumped upward through the expansion section of the flow cell. The flow was stopped before imaging, so that the images are stationary. The ratio of isooctane to 1,6 dibromohexane contained in the emulsion beads was chosen so as to match the density of the suspending fluid and the polystyrene particles, in order to eliminate gravitational effects in the flow. Minor density differences between the polystyrene particles and the other components did not cause significant motion during image acquisition, but led to slow

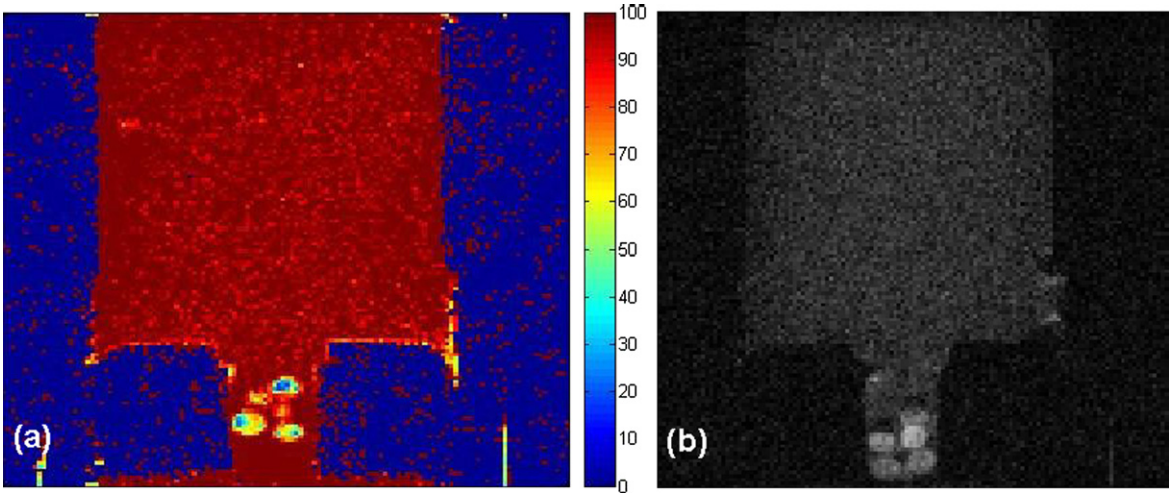

Fig. 6. Longitudinal views of oil-in-water alginate emulsion beads as tracer particles in a suspension flowing through the expansion section of an abrupt 4:1:4 annular contraction–expansion. Both images shown have FOV = 3 cm × 3 cm and 128 × 128 pixel. (a) T_2 relaxation time map (scale indicates 0–100 ms) obtained from CPMG pulse sequence with TR = 2 s, TE = 5.37 ms, 25 echoes, slice thickness = 0.5 mm; (b) stimulated echo diffusion weighted image, diffusion gradient = 66.67 mT/m, TR = 2 s, TE = 11.5 ms, $\Delta = 400$ ms, $\delta = 1$ ms, slice thickness = 1.5 mm.

settling of the polystyrene particles, and affected the location of the emulsion beads in the flow cell during long static intervals. During flow, however, hydrodynamic forces from the viscous suspension dominated the weak gravitational effects, which could be neglected. In future flow studies, the ratio of isooctane to 1,6 dibromohexane may be altered to optimize the density matching. In Fig. 6(a), a T_2 map is shown, and the emulsion beads can be seen in the narrow inlet tube. The image demonstrates the feasibility of using alginate beads as a tracer particle based on differing T_2 relaxation times.

Fig. 6(b) is a stimulated echo diffusion weighted image taken shortly thereafter. The scan parameters were identical to those used for the image in Fig. 2(c), except that the diffusion gradient strength was lower, at 66.67 mT/m. The emulsion beads had moved slightly due to imperfect density matching of the polystyrene particles. The image shows that a diffusion weighted image strongly differentiates the emulsion beads from the other materials.

In addition to use as tracer particles, alginate gel beads can also be used in experiments that involve mixtures of two or more particle sizes, where the alginate gel particles may occupy a significant fraction of the solid portion of the suspension, and the relative volume fractions can be dramatically varied. In order to distinguish between rigid polymer particles and alginate (either plain or emulsion) beads, T_2 relaxation time contrast can be utilized between the rigid particles, alginate gel (either plain or emulsion) beads, and suspending fluid. The total particle volume fraction can be obtained from spin-echo images at long echo times [25,26], and double exponential fitting of a multi-echo series in each pixel can determine the relative volume fractions of fluid and alginate particles, after calibration. Alginate gel beads that are smaller than the image pixel dimensions can be employed as long as the desired measurement is the average volume fraction in each pixel. If concentration profiles are desired for more than two particle types, further distinction between alginate emulsion beads and plain alginate beads is available through diffusion contrast. The results obtained from such a method can be used to establish guidelines for particle size separations and bimodal suspension microstructure in complex flow geometries such as the abrupt annular expansion.

4. Conclusions

We have demonstrated that alginate emulsion microbeads are feasible as contrast agents for the study of the flow properties of fluids using nuclear magnetic resonance imaging. Results indicate that combined spin–spin (T_2) relaxation and diffusion contrast in proton NMR imaging can be used to distinguish among rigid polymer particles, plain alginate beads, and alginate emulsion beads. The alginate beads are produced by simple ionic gelation and do not require detailed chemical synthesis. Also, the versatility of the emulsion bead production method allows custom tailoring of the particle size and density. Multi-echo CPMG spin-echo imaging indicates that the average T_1 and T_2 relaxation times of the plain alginate and alginate emulsion beads are comparable. Meanwhile, diffusion weighted imaging produces sharp contrast between the two types of alginate beads, due to restricted diffusion inside the embedded oil droplets of the alginate emulsion beads. When the alginate emulsion beads were added to a suspension and imaged in an abrupt annular expansion flow, the emulsion beads could be clearly distinguished from the surrounding suspending fluid and rigid polystyrene particles, through either T_2 relaxation or diffusion contrast. Such a capability allows future use of the alginate emulsion beads as tracer particles and as one particle type among many in a multimodal suspension where detailed concentration profiles

or particle size separation must be quantified during flow.

Acknowledgments

The authors gratefully acknowledge financial support from NYSTAR (#C030109), and thank the Hatch NMR Research Center of the Radiology Department at Columbia University Medical Center.

References

[1] M. George, T.E. Abraham, Polyionic hydrocolloids for the intestinal delivery of protein drugs: alginate and chitosan—a review, Journal of Controlled Release 114 (2006) 1–14.
[2] W. Krasaekoopt, B. Bhandari, H. Deeth, The influence of coating materials on some properties of alginate beads and survivability of microencapsulated probiotic bacteria, International Dairy Journal 14 (2004) 737–743.
[3] B.F. Gibbs, S. Kermasha, I. Alli, C.N. Mulligan, Encapsulation in the food industry: a review, International Journal of Food Sciences and Nutrition 50 (1999) 213–224.
[4] G. Coppi, V. Iannuccelli, M.T. Bernabei, R. Cameroni, Alginate microparticles for enzyme peroral administration, International Journal of Pharmaceutics 242 (2002) 263–266.
[5] J.-O. You, C.-A. Peng, Calcium-alginate nanoparticles formed by reverse microemulsion as gene carriers, Macromolecular Symposia 219 (2005) 147–153.
[6] M.N.V.R. Kumar, Nano and microparticles as controlled drug delivery devices, Journal of Pharmacy and Pharmaceutical Sciences 3 (2000) 234–258.
[7] N. Nestle, R. Kimmich, Heavy metal uptake of alginate gels studied by NMR microscopy, Colloids and Surfaces A: Physicochemical and Engineering Aspects 115 (1996) 141–147.
[8] A. Blandino, M. Macias, D. Cantero, Glucose oxidase release from calcium alginate gel capsules, Enzyme and Microbial Technology 27 (2000) 319–324.
[9] H. Zhu, R. Srivastava, J.Q. Brown, M.J. McShane, Combined Physical and Chemical Immobilization of Glucose Oxidase in Alginate Microspheres Improves Stability of Encapsulation and Activity, Bioconjugate Chemistry 16 (2005) 1451–1458.
[10] P. De Vos, B. De Haan, R. Van Schilfgaarde, Effect of the alginate composition on the biocompatibility of alginate–polylysine microcapsules, Biomaterials 18 (1997) 273–278.
[11] K. Potter, T.A. Carpenter, L.D. Hall, Mapping of the spatial variation in alginate concentration in calcium alginate gels by magnetic resonance imaging (MRI), Carbohydrate Research 246 (1993) 43–49.
[12] B. Thu, O. Gåserød, D. Paus, A. Mikkelson, G. Skjåk-Bræk, R. Toffanin, F. Vittur, R. Rizzo, Inhomogenous alginate gel spheres: an assessment of the polymer gradients by synchrotron X-ray emission, magnetic resonance microimaging, and mathematical modelling, Biopolymers 53 (2000) 60–71.
[13] N.E. Simpson, S.C. Grant, S.J. Blackband, I. Constantinidis, NMR properties of alginate microbeads, Biomaterials 24 (2003) 4941–4948.
[14] N.C. Shapley, M.A. d'Avila, Two-phase flow of emulsions, in: S. Stapf, S.-I. Han (Eds.), Nuclear Magnetic Resonance Imaging in Chemical Engineering, Weinheim, Germany, 2006, pp. 433–456.
[15] S.L. Codd, P.T. Callaghan, Spin echo analysis of restricted diffusion under generalized waveforms: planar, cylindrical, and spherical pores with wall relaxivity, Journal of Magnetic Resonance 137 (1999) 358–372.
[16] N.C. Shapley, M.A. d'Avila, J.H. Walton, R.L. Powell, S.R. Dungan, R.J. Phillips, Complex flow transitions in a homogeneous, concentrated emulsion, Physics of Fluids 15 (2003) 881–891.
[17] M.A. d'Avila, N.C. Shapley, J.H. Walton, R.J. Phillips, R.L. Powell, S.R. Dungan, A novel gravity-induced flow transition in two-phase fluids, Physics of Fluids 18 (2006) 103305.
[18] J.D. Seymour, A. Caprihan, S.A. Altobelli, E. Fukushima, Pulsed gradient spin echo nuclear magnetic resonance imaging of diffusion in granular flow, Physical Review Letters 84 (2000) 266–269.
[19] M. Nakagawa, S.A. Altobelli, A. Caprihan, E. Fukushima, E.K. Jeong, Noninvasive measurements of granular flows by magnetic-resonance-imaging, Experiments in Fluids 16 (1993) 54–60.
[20] H. Wassenius, M. Nyden, B. Vincent, NMR diffusion studies of translational properties of oil inside core-shell latex particles, Journal of Colloid and Interface Science 264 (2003) 538–547.
[21] H. Wassenius, P.T. Callaghan, Nanoscale NMR velocimetry by means of slowly diffusing tracer particles, Journal of Magnetic Resonance 169 (2004) 250–256.
[22] H. Wassenius, P.T. Callaghan, NMR velocimetry studies of the steady-shear rheology of a concentrated hard-sphere colloidal system, European Physical Journal 18 (2005) 69–84.
[23] U. Noth, L.M. Rodrigues, S.P. Robinson, A. Jork, U. Zimmermann, B. Newell, J.R. Griffiths, In vivo determination of tumor oxygenation during growth and in response to carbogen breathing using 15C5-loaded alginate capsules as fluorine-19 magnetic resonance imaging oxygen sensors, International Journal of Radiation Oncology Biology Physics 60 (2004) 909–919.
[24] J.O. You, S.B. Park, H.Y. Park, S. Haam, C.H. Chung, W.S. Kim, Preparation of regular sized Ca-alginate microspheres using membrane emulsification method, Journal of Microencapsulation 18 (2001) 521–532.
[25] T. Moraczewski, H. Tang, N.C. Shapley, Flow of a concentrated suspension through an abrupt axisymmetric expansion measured by nuclear magnetic resonance imaging, Journal of Rheology 49 (2005) 1409–1428.
[26] T. Moraczewski, N.C. Shapley, The effect of inlet conditions on concentrated suspension flows in abrupt expansions, Physics of Fluids 18 (2006) 123303.
[27] H.T. Edzes, D. van Dusschoten, H. Van As, Quantitative T-2 imaging of plant tissues by means of multi-echo MRI microscopy, Magnetic Resonance Imaging 16 (1998) 185–196.
[28] P. McConville, J.M. Pope, ^{1}H NMR T2 relaxation in contact lens hydrogels as a probe of water mobility, Polymer 42 (2001) 3559–3568.
[29] M.A. d'Avila, R.L. Powell, R.J. Phillips, N.C. Shapley, J.H. Walton, S.R. Dungan, Magnetic resonance imaging (MRI): a technique to study flow and microstructure of concentrated emulsions, Brazilian Journal of Chemical Engineering 22 (2005) 49–60.
[30] K.G. Hollingsworth, M.L. Johns, Spatially resolved emulsion droplet sizing using inverse Abel transforms, Journal of Magnetic Resonance 176 (2005) 71–78.